Progress In Electromagnetics Research C, Vol. 113, 197–209, 2021

Design of Triple Band-Notched UWB MIMO/Diversity Antenna Using Triple Bandgap EBG Structure

Priyanka Dalal* **and Sanjeev K. Dhull**

Abstract—This paper presents the design of a compact triple band-notched ultra-wideband (UWB) two element multiple-input multiple-output (MIMO) antenna. To validate the simulation results, the prototype of the design is fabricated and experimentally measured. From the experimental results, it is observed that the proposed design, operating in the frequency range 2.5–12 GHz, successfully rejects three interfering bands, i.e., the WiMAX band, WLAN band, and X-band satellite communication downlink channel, when a triple bandgap CSRR-loaded EBG structure is embedded close to the feedline of the UWB antenna. In the ground plane of the MIMO antenna, a rectangular slot and a mirrored pair of F-shaped stubs are added to minimize the mutual coupling between the UWB elements. The proposed MIMO antenna has good wideband isolation between the elements (> 20 dB), high diversity gain (10 dB), and low envelope correlation coefficient (< 0.02) over the entire UWB.

1. INTRODUCTION

In the year 2002, the band ranging from 3.1 to 10.6 GHz was approved and allocated by the Federal Communications Commission (FCC) for ultra-wideband (UWB) technology [1]. Since then, many researchers and engineers have been attracted towards developing RF circuits and antennas for this technology. UWB technology aims to provide short-range indoor wireless communications at a high data rate [2]. For the successful deployment of UWB technology low-profile antennas with ultra-wide bandwidth, high radiation efficiency, stable gain, and stable radiation pattern are required. Printed monopole antennas with a partial ground plane have been the most promising candidate for UWB technology since these antennas have low profile, low cost, easy fabrication, and large bandwidth [3–7].

However, some existing narrow-band systems operating at higher power levels interfere in the operating frequency range of UWB technology. These narrow-band systems include Worldwide Interoperability for Microwave Access (WiMAX) operating in range 3.4–3.69 GHz, Wireless Local Area Network (WLAN) operating in range 5.15–5.825 GHz, X-band satellite communication operating in range 7.25–7.75 GHz (downlink channel), and 7.9–8.4 GHz (uplink channel). To mitigate such interferences, additional band-reject filters are required to be included in the system. However, such filters increase the overall cost, size, and complexity of the system. An alternative method is to design band-notched UWB antennas that will automatically discard the interfering bands [8–14]. In the literature, several methods have been proposed to obtain band-notched UWB antennas. These methods include adding slots in the radiating patch or the ground plane [8–12], putting parasitic elements [13, 14] or tuning stubs [15] near the radiating patch, or embedding resonant structures near/on the microstrip feedline [16, 17]. To achieve multiple band-notched functionality, adding multiple stubs/tuning structures would not be practical because they will consume more space and can present strong coupling effects. Also, it would be very challenging to add more than three slots in the radiating patch because a compact UWB antenna has a very limited patch area. Multiple slots in the radiating

Received 2 May 2021, Accepted 23 June 2021, Scheduled 25 June 2021
* Corresponding author: Priyanka Dalal (priyanka.dalal17@gmail.com).
The authors are with the Department of Electronics and Communication Engineering, Guru Jambheshwar University of Science and Technology, Hisar, India.

patch will also affect the gain, efficiency, and radiation pattern of the antenna. Moreover, these band-notch techniques are restricted to a specific design of a monopole antenna and may not be reused to achieve band-notch functionality in any other monopole antenna design.

Another technique that has been recently used by the authors to obtain band rejection is placing Electromagnetic Band Gap (EBG) structures close to the microstrip feedline of the monopole antenna [18–26]. EBG structures perform band-notch in the UWB spectrum at their bandgap resonant frequency [18]. EBG structures also offer the flexibility to tune the bandwidth and center frequency of the notched band easily [19]. Moreover, these structures have a minimal affect on the radiation characteristics of the UWB antenna and can be easily coupled close to the microstrip feedline of the monopole antenna, independent of its design. Four Conventional Mushroom Type (CMT) EBG structures were utilized in [18] to obtain a notch in the spectrum of UWB monopole antenna at 5.5 GHz. In [19], to notch the WLAN band, a comparative study of CMT EBG and Edge Located Via (ELV) EBG was performed. Three different EBG structures were utilized in [20] and [21] to obtain a triple band-notched UWB antenna. However, the ground plane of a UWB monopole antenna is limited. For miniaturized portable hand-held wireless electronic devices, there is a demand for more compact UWB antennas. For a compact UWB antenna, the ground plane area is further reduced. It would be very difficult to accommodate in the limited ground plane area, the unit cells of three/four different sized EBG structures to design triple/quad band-notched UWB antenna [22]. Hence recently many authors have proposed UWB antennas integrated with dual/triple bandgap EBG structures [23–28] so that a single cell of EBG structure may suffice the requirement. However, all these structures have complicated designs and are difficult to fabricate.

In recent years, multiple-input multiple-output (MIMO) systems have also gained popularity because of their ability to improve channel capacity, data rate, and link reliability without any additional spectral resources [29]. MIMO systems comprise multiple antenna elements at the transmitter and receiver. MIMO technology, when being combined with UWB technology, helps in further improving the data rate and channel capacity of UWB technology. A UWB MIMO/Diversity antenna is an appropriate candidate to combat the multipath fading problem in indoor environments. However since a MIMO antenna consists of multiple individual antenna elements, the overall size of a UWB MIMO antenna increases. Thus, there is a need to design compact UWB MIMO antennas that can be easily accommodated within compact portable hand-held wireless devices. For a UWB MIMO system to operate well, low correlation and mutual coupling between the individual antenna elements are desired. Several decoupling methods have been reported in the literature [29–42] to minimize the mutual coupling between the antenna elements.

In this paper, a compact triple band-notched UWB MIMO antenna system comprising two fork-shaped UWB antenna elements is proposed. The overall footprint of the MIMO antenna is $30 \times 44\,\text{mm}^2$. To obtain the notches in the UWB antenna bandwidth, a triple bandgap EBG structure is proposed and embedded close to the microstrip feedline of the UWB antenna. To minimize the mutual coupling between the MIMO elements, a mirrored pair of F-shaped stubs and one rectangular slot are added in the common ground plane. Section 2 discusses the design of the fork-shaped UWB monopole antenna. Section 3 presents the dispersion diagram of the triple bandgap CSRR-loaded EBG structure. The triple band-notched UWB monopole antenna is studied in Section 4. Section 5 presents the design of the two-element UWB MIMO/Diversity antenna. Measurement results of UWB MIMO/Diversity antenna are presented and discussed in Section 6. Finally, the paper is concluded in Section 7.

2. DESIGN OF THE UWB ANTENNA

A microstrip-fed monopole antenna with a fork-shaped radiating patch and a partial ground plane is used as a reference UWB antenna [43]. The top view and side view of the antenna are presented in Figures 1(a) and (b), respectively. The antenna is designed on a low-cost FR4 epoxy substrate with dielectric constant $(\epsilon_r) = 4.4$, loss tangent $(\tan\delta) = 0.01$, and substrate height $(h) = 1.6\,\text{mm}$. Ansys High Frequency Structure Simulator (HFSS) is used to optimize the dimensions of the antenna. Return loss and other characteristics of the antenna are also studied using the simulations performed in HFSS. The final optimized parameters of the antenna are $L = 30\,\text{mm}$, $W = 20\,\text{mm}$, $L1 = 12.5\,\text{mm}$, $L2 = 2\,\text{mm}$, $Lf = 11.5\,\text{mm}$, $W1 = 2\,\text{mm}$, $W2 = 11\,\text{mm}$, $Wf = 3.4\,\text{mm}$. The overall footprint of the

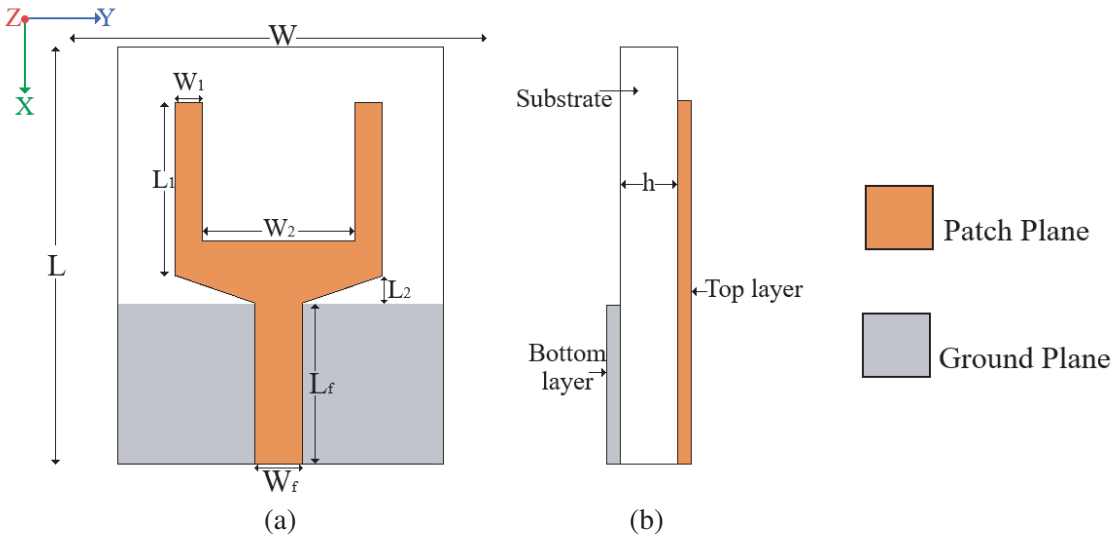

Figure 1. Fork shaped UWB antenna. (a) Top view, (b) side view.

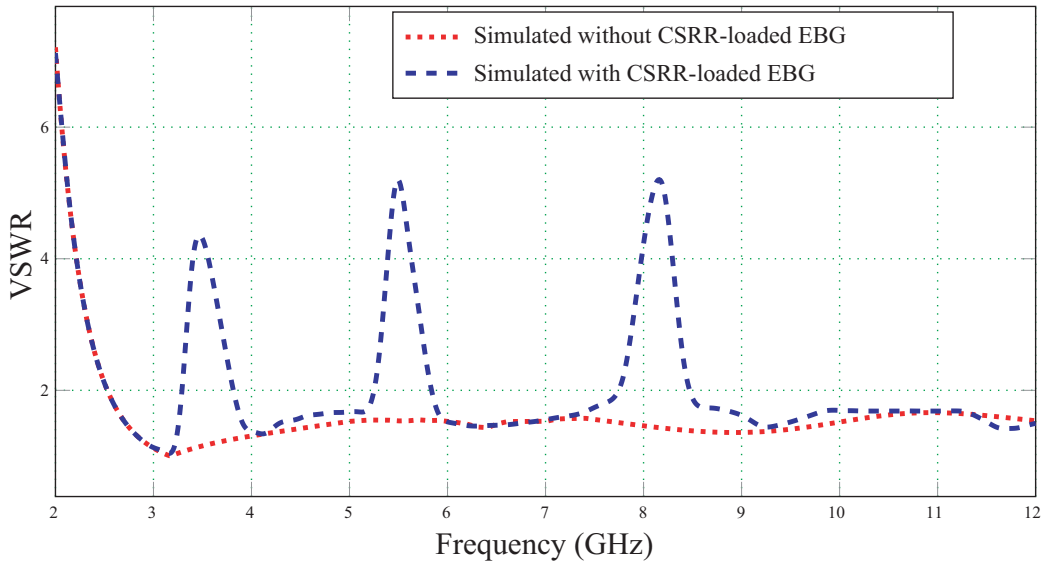

Figure 2. Simulated VSWR of fork-shaped UWB antenna.

antenna is $30 \times 20\,\text{mm}^2$. The simulated VSWR of the antenna is presented in Figure 2. From Figure 2, it is observed that the simulated bandwidth of the antenna with VSWR < 2 is from 2.5 GHz to 12 GHz.

3. DESIGN OF TRIPLE BANDGAP EBG STRUCTURE

EBG structures are periodic metallic patches arranged over dielectric substrates [44]. Because of the two unique characteristics of EBG structures, i.e., surface wave bandgap and reflection phase bandgap, these structures have been exploited by microwave and antenna engineers for a vast number of applications [45, 46]. To explain the characteristics of EBG structures, the unit cell of via loaded EBG structure can be equated to an equivalent LC circuit, where the inductance L is accounted to the current flowing through the via, and the capacitance C is accounted to the gap between the EBG patches. The

bandgap is observed at the resonant frequency of this LC circuit. To design a multi-bandgap EBG structure, multiple LC resonant circuits must be observed per unit cell of an EBG structure.

When a unit cell of the EBG structure is placed close to the microstrip feedline of a UWB antenna, notch/notches are observed in the operating bandwidth of the UWB antenna. These notch/notches coincide with the bandgap/bandgaps of the EBG structure. To obtain the triple notches in the bandwidth of the fork-shaped UWB antenna proposed in the above section, placing the unit cell of the triple bandgap EBG structure near the microstrip feedline will suffice. Hence in this section, we aim to design a triple bandgap EBG structure with optimized dimensions so that it offers bandgap at the WiMAX band 3.4–3.69 GHz, WLAN band 5.15–5.825 GHz, and X-band 7.9–8.4 GHz.

The top view and side view of the proposed CSRR-loaded EBG structure are presented Figures 3(a) and (b), respectively. The proposed EBG structure is square-shaped loaded with two complementary split-ring resonators (CSRR) and an edge via. The design of this EBG structure is inspired from the reference [47]. The two CSRRs offer two additional resonances to the unit cell. Hence, three resonant circuits and consequently three bandgaps are observed per unit cell. The CSRR-loaded EBG structure is designed on an FR4 substrate with dielectric constant $(\epsilon_r) = 4.4$, loss tangent $(\tan\delta) = 0.01$, and substrate height $(h) = 1.6\,\text{mm}$. The optimized dimensions of the EBG structure are: patch size $x1 = 7.3\,\text{mm}$, Period of EBG structure $P = 8.1\,\text{mm}$ (where $P = x1{+}2{\times}g$), gap between the neighbouring cells $= 2 \times g = 0.8\,\text{mm}$, $x2 = 5.5\,\text{mm}$, $x3 = 3.7\,\text{mm}$, $g1 = 0.5\,\text{mm}$, $g2 = 0.5\,\text{mm}$, and radius of via $= 0.2\,\text{mm}$. Figure 3(c) presents the dispersion diagram (from τ to X) of the CSRR-loaded EBG structure drawn using rectangular irreducible Brillouin-zone. From the dispersion diagram, it is observed that the CSRR-loaded EBG structure offers three bandgaps. The first bandgap observed between mode-1 and mode-2 is 3.32–3.78 GHz, centered at $f_{c1} = 3.55\,\text{GHz}$. The second bandgap observed between mode-2 and mode-3 is 5.36–5.81 GHz, centered at $f_{c2} = 5.58\,\text{GHz}$. The third bandgap observed between mode-3 and mode-4 is 7.84–8.35 GHz, centered at $f_{c3} = 8.08\,\text{GHz}$. The fractional bandwidths of the three bandgaps are 12.95%, 8.6%, and 6.5%, respectively.

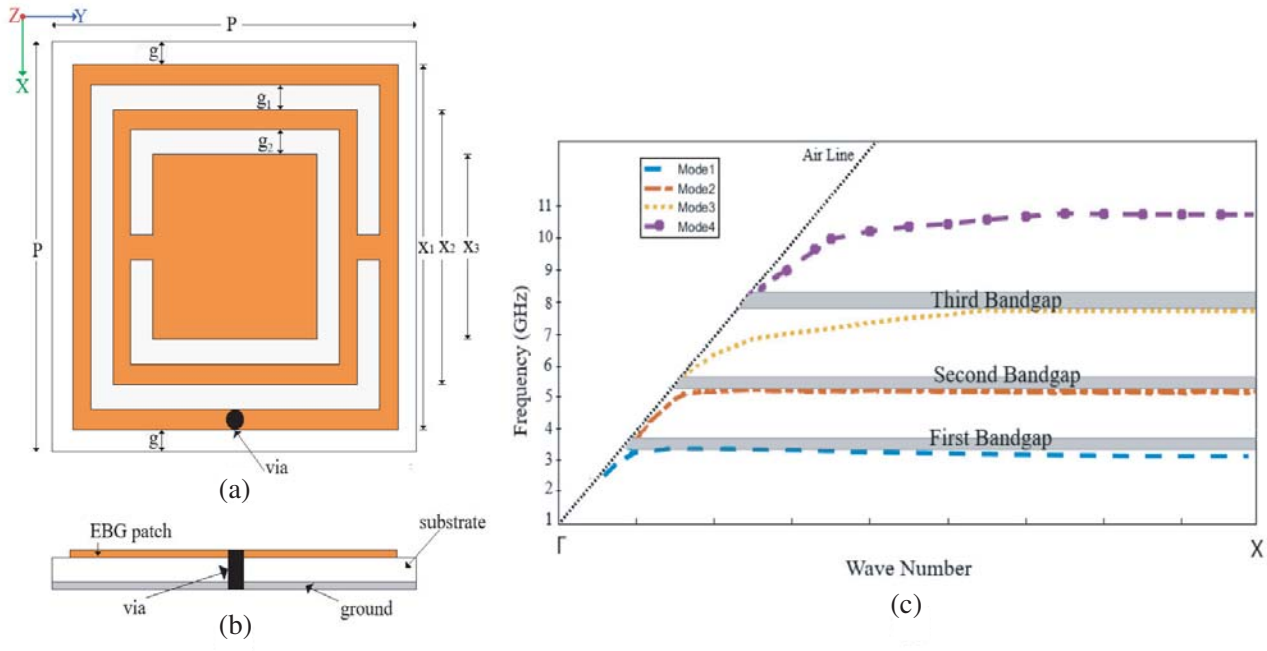

Figure 3. CSRR-loaded EBG structure. (a) Top view, (b) side view, (c) dispersion diagram.

4. DESIGN OF TRIPLE BAND-NOTCHED UWB ANTENNA

In this section, the CSRR-loaded EBG structure is placed at a distance of $d2$ from the microstrip feedline of the UWB antenna. The dimensions of the CSRR-loaded EBG structure are taken the same

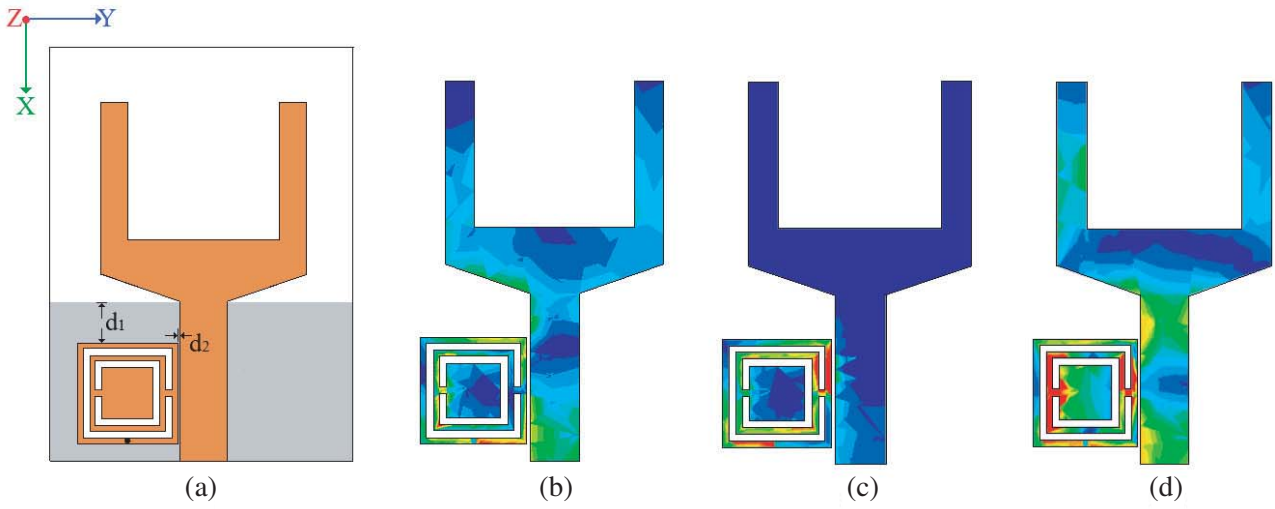

Figure 4. EBG integrated UWB antenna. (a) Top view, (b) current distribution at 3.4 GHz, (c) current distribution at 5.5 GHz, (d) current distribution at 8.2 GHz.

as discussed in Section 3. Figure 4(a) presents the top view of the EBG integrated antenna. The distance between the upper edge of the ground plane and the EBG structure is $d1$. The distances $d1$ and $d2$ play an important role in fine-tuning the center frequency and the bandwidth of the notched band. With the help of HFSS simulations, the most optimum values of $d1$ and $d2$ are observed as $d1 = 3$ mm and $d2 = 0.2$ mm. Figure 2 presents the simulated VSWRs of UWB antenna without any EBG structure and after embedding the CSRR-loaded EBG structure. It is observed from the figure that three bands are notched (with VSWR > 2) from the operating bandwidth of the EBG integrated antenna. The first notched band is 3.3–3.8 GHz, the second notched band 5.32–5.85 GHz, and third notched band 7.8–8.41 GHz. These notched bands coincide closely with the bandgaps observed in the dispersion diagram of the CSRR-loaded EBG structure. Figures 4(b), (c), and (d) respectively present the simulated surface current distributions at the antenna and the EBG structure at 3.4 GHz, 5.5 GHz, and 8.2 GHz. At the notched frequencies, current is observed to be concentrated more at the EBG structure. Table 1 presents the comparison of CSRR-loaded EBG structure with other reported EBG

Table 1. Comparison of the CSRR-loaded EBG structure with other reported EBG structures.

Ref. No.	EBG Type	unit cell size (mm^2)	No. of vias/unit cell	No. of bandgaps	bandgap center frequency $f_{c1}/f_{c2}/f_{c3}$ (GHz)	cell size in terms of λ of first bandgap center frequency
[23]	M-EBG	8 × 8.2	one	two	3.6/5.5	$0.096\lambda_{c1} \times 0.098\lambda_{c1}$
[24]	CMT EBG with slits	4.5 × 4.5	one	two	5.5/8.2	$0.083\lambda_{c1} \times 0.083\lambda_{c1}$
[25]	Slotted EBG	9.5 × 4.5	one	three	3.63/5.48/7.35	$0.115\lambda_{c1} \times 0.055\lambda_{c1}$
[26]	TVEL EBG	6 × 6	two	two	3.9/7.45	$0.078\lambda_{c1} \times 0.078\lambda_{c1}$
[27]	TVDS EBG	11 × 11	two	two	4.54/5.92	$0.166\lambda_{c1} \times 0.166\lambda_{c1}$
[28]	TBMV EBG	12 × 12	three	three	2.17/3.73/4.77	$0.086\lambda_{c1} \times 0.086\lambda_{c1}$
P.W.	CSRR-loaded	7.3 × 7.3	one	three	3.4/5.5/8.2	$0.083\lambda_{c1} \times 0.083\lambda_{c1}$

P.W. = Proposed Work

structures that have been utilized to obtain notches in the bandwidth of UWB antennas. From Table 1, it is observed that the CSRR-loaded EBG structure is multi-bandgap, and as compared to other reported EBG structures more compact, and simpler to fabricate.

5. DESIGN OF TRIPLE BAND-NOTCHED UWB MIMO/DIVERSITY ANTENNA

With the help of MIMO technology, the problem of multipath fading in conventional UWB systems can be resolved. This technology also helps to improve the quality of transmission. In this section, two UWB monopoles along with two CSRR-loaded EBG structures are placed on a common FR4 substrate to obtain a two-port UWB MIMO/Diversity antenna system. To minimize the mutual coupling among the UWB monopoles, a mirrored pair of F-shaped stubs are added to the common ground plane. These F-shaped stubs act as a reflector and separate the radiation of each monopole, thus reducing the mutual coupling between the antenna elements [35]. To further reduce the mutual coupling, a rectangular slot is also added in the middle of the ground plane. Figure 5(a) presents the layout of the proposed MIMO antenna. The dimensions of the F-shaped stub are as follows: $a = 8\,\text{mm}$, $b = 1.5\,\text{mm}$, $c = 0.4\,\text{mm}$, $d = 1\,\text{mm}$, and $e = 3\,\text{mm}$. The slot dimensions are: $m = 4\,\text{mm}$, $n = 2\,\text{mm}$. The other dimensions of the UWB monopoles and EBG structures are same as discussed in the above sections. The overall footprint of the proposed MIMO/Diversity antenna is $30 \times 44\,\text{mm}^2$. Figure 5(b) presents the surface current distribution on the ground plane of MIMO antenna at 5 GHz, when Port 1 is excited. From the figure it is observed that the current coupled to the second monopole antenna is very small. Thus, it can be concluded that good isolation is achieved between the radiators.

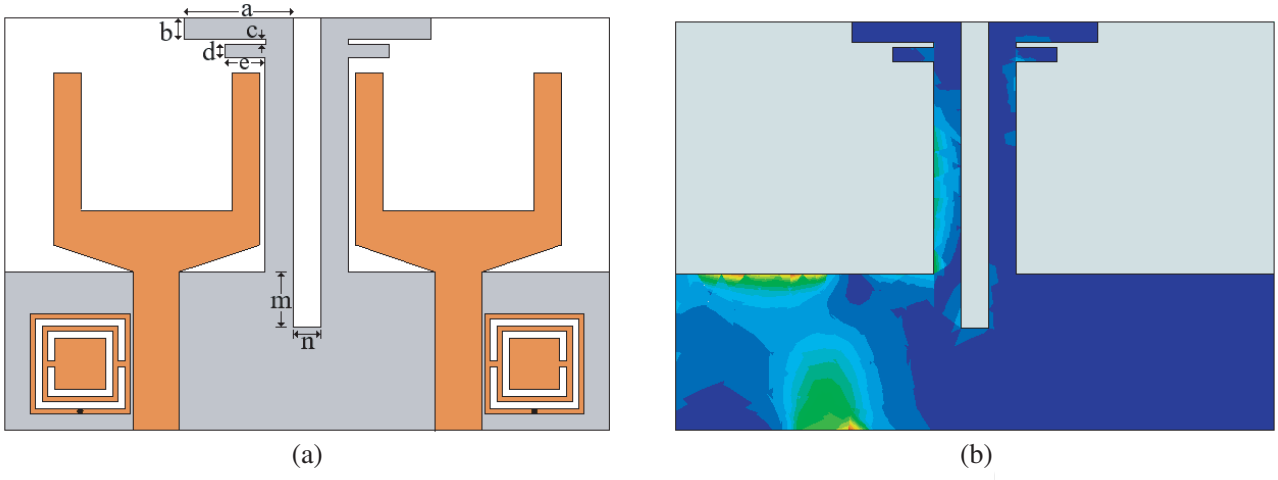

Figure 5. UWB MIMO antenna. (a) Top view, (b) ground plane surface current distribution.

6. RESULTS AND DISCUSSION

To validate the performance, the proposed UWB MIMO antenna is fabricated on an FR4 substrate with dielectric constant $(\epsilon_r) = 4.4$, substrate height $= 1.6\,\text{mm}$, and loss tangent $(\tan\delta) = 0.01$. The front and back views of the fabricated prototype are shown in Figure 6. At the end of the microstrip feedline of each UWB monopole, two $50\,\Omega$ SMA connectors are connected. For all the measurements Port 1 is excited, while Port 2 is terminated with a $50\,\Omega$ load.

6.1. Return Loss and Mutual Coupling

Figure 6 compares the simulated and measured return loss values of the UWB MIMO antenna. It is observed from the graph that the measurement results closely follow the simulation results. However, minor variations are observed, which can be attributed to the soldering of the SMA connector and

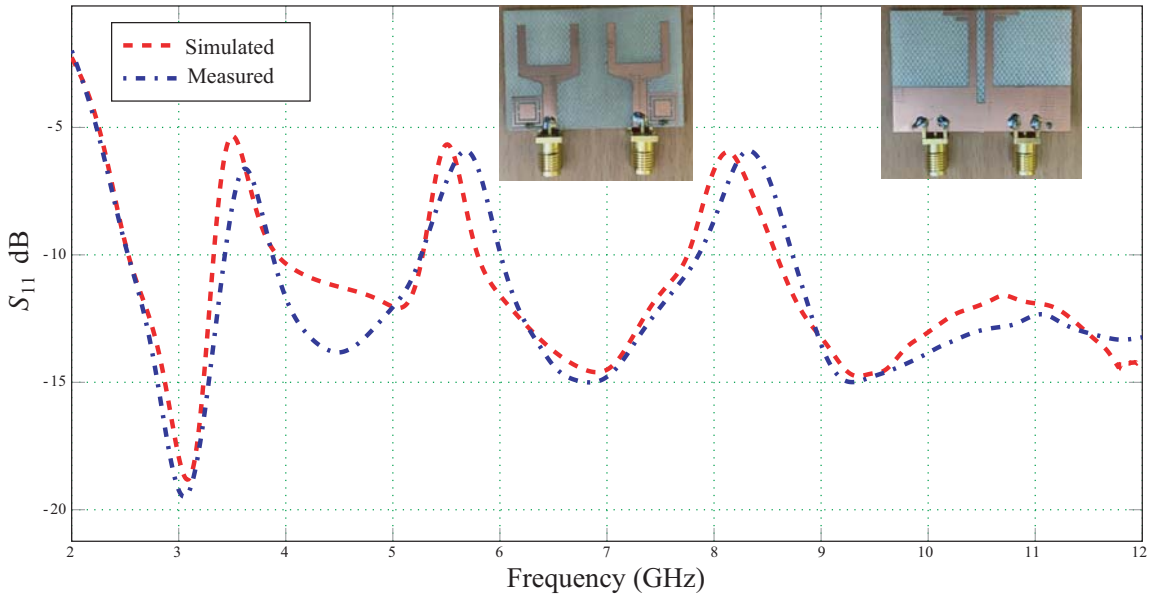

Figure 6. Simulated and measured S_{11} of UWB MIMO antenna and photograph of fabricated prototype.

fabrication tolerances. From the measurement results, it is observed that the impedance bandwidth of the fabricated prototype ($S_{11} < -10$ dB) is from 2.5 GHz to 12 GHz, while the antenna simultaneously rejects three interfering frequency bands ($S_{11} > -10$ dB) from 3.43–3.86 GHz, 5.26–6 GHz, and 7.85–8.71 GHz.

The mutual coupling between the antenna elements is measured in terms of transmission coefficient from Port 1 to Port 2 or vice versa, i.e., S_{12}/S_{21}. Figure 7 compares the simulated and measured transmission coefficient values. It is observed that throughout the entire UWB, the value of S_{21} is less than -20 dB which is considered acceptable for a good performance. Thus the decoupling structures, i.e., the F-shaped stubs and slot in the common ground plane helped in a significant reduction of mutual coupling.

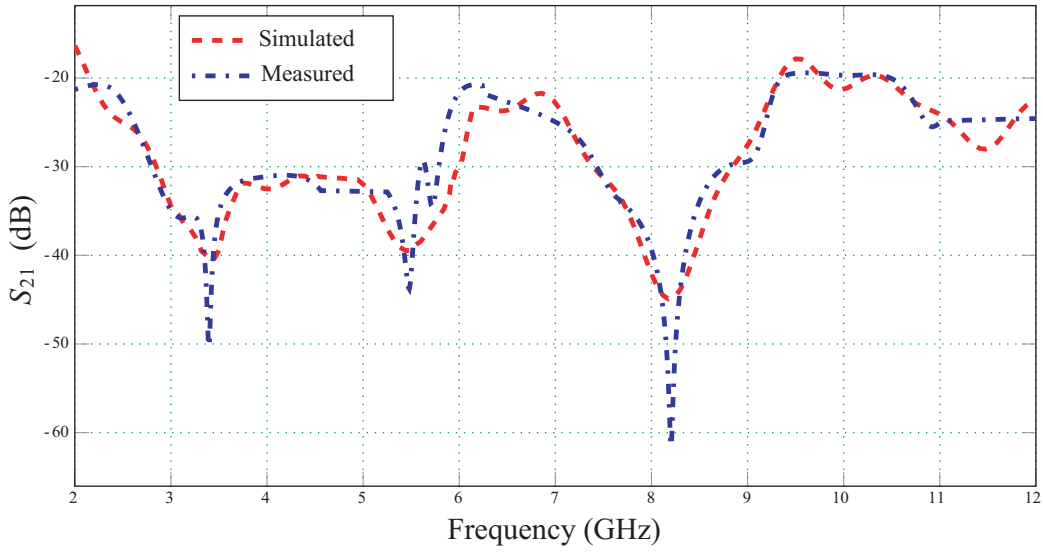

Figure 7. Simulated and measured mutual coupling (S_{21}) of the proposed UWB MIMO antenna.

6.2. Radiation Pattern and Gain

In an anechoic chamber, the far-field radiation performance of the fabricated antenna is measured. At three dissimilar frequencies, the simulated and measured E-plane and H-plane radiation patterns of the MIMO antenna are presented in Figure 8. A good agreement between simulated and measured results has been observed. The radiation pattern of the proposed MIMO antenna is dumbbell-shaped in the E-plane and almost omnidirectional in the H-plane. Such a radiation pattern is typical for a monopole antenna. However, at higher frequencies some deterioration is observed in the radiation pattern.

Figure 9 presents simulated peak gain graph of the proposed MIMO antenna varying with frequency. It is observed that the gain of the antenna is acceptable for the entire UWB except at the notched frequency bands where a sharp decrease in antenna gain is observed.

6.3. Envelope Correlation Coefficient and Diversity Gain

The diversity performance of the proposed antenna is evaluated in terms of Envelope Correlation Coefficient (ECC) and Diversity Gain (DG). The formula for the evaluation of ECC of the MIMO

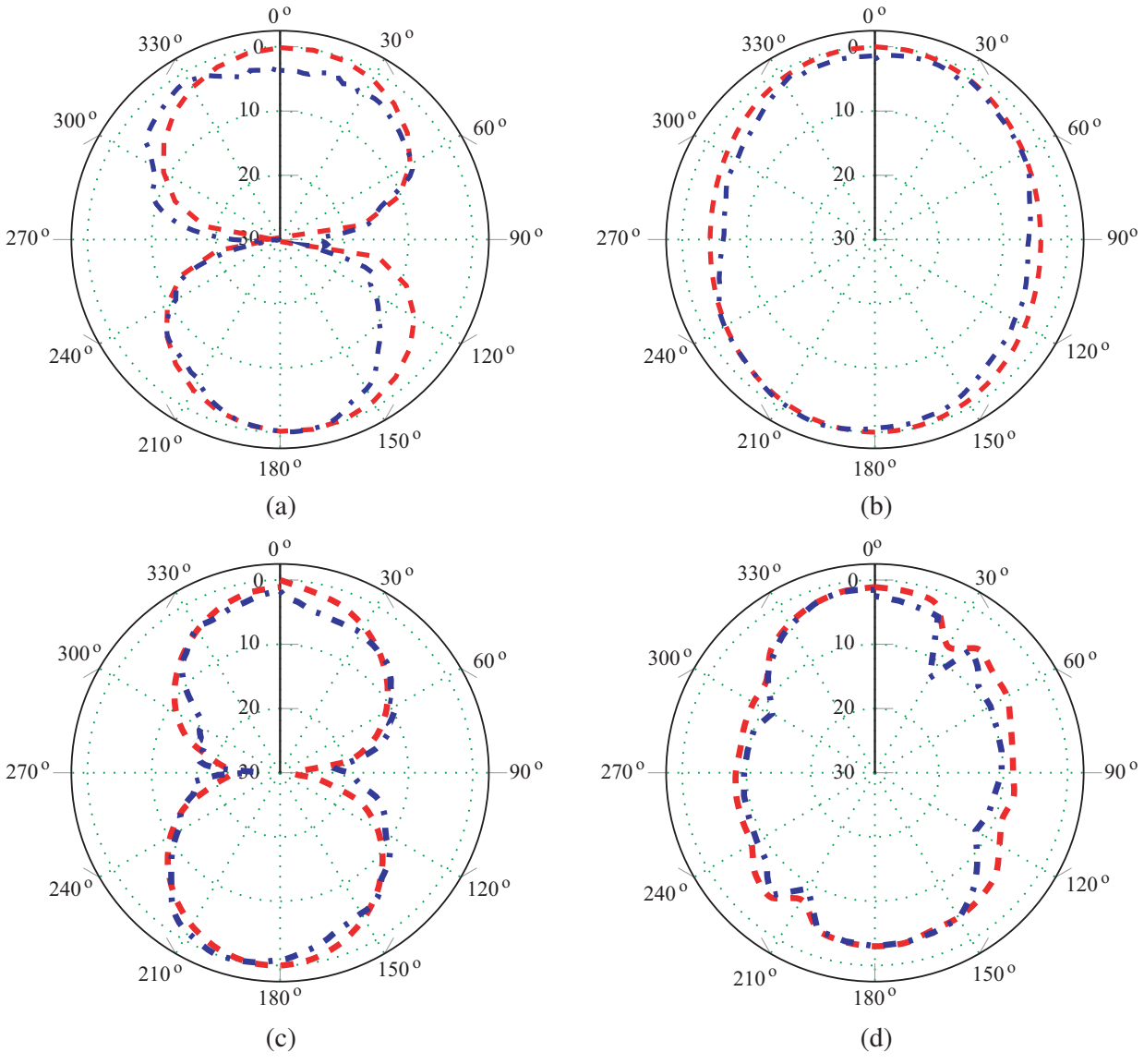

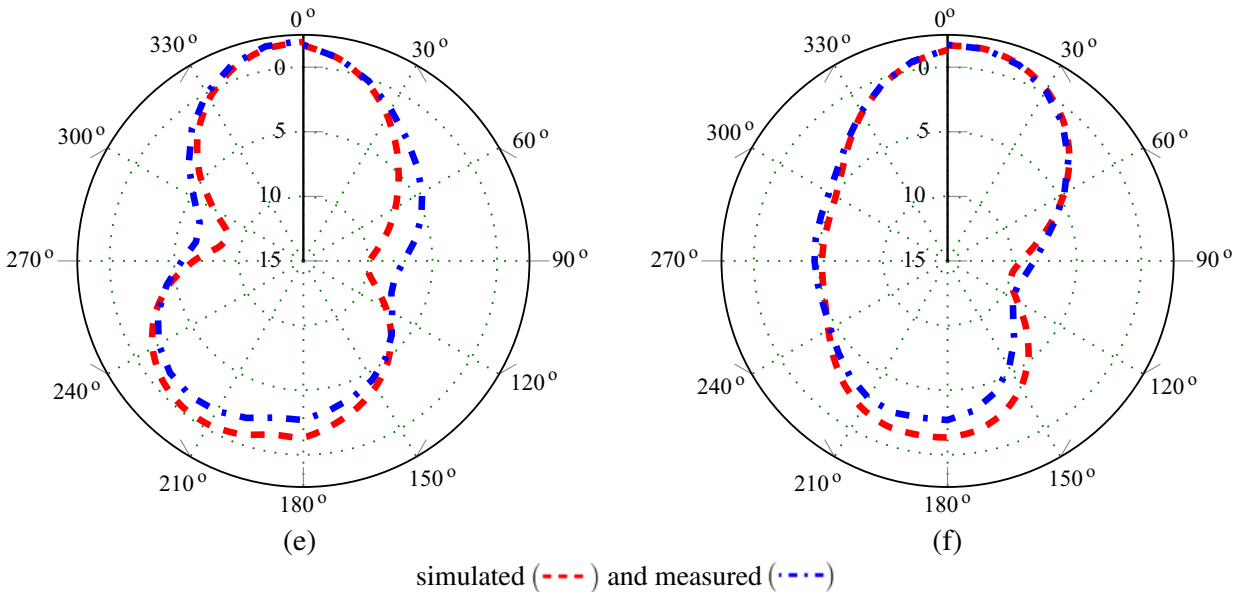

Figure 8. Simulated and measured radiation patterns of proposed UWB MIMO antenna. (a) E-plane at 4.5 GHz, (b) H-plane at 4.5 GHz, (c) E-plane at 6.5 GHz, (d) H-plane at 6.5 GHz, (e) E-plane at 9.5 GHz, (f) H-plane at 9.5 GHz.

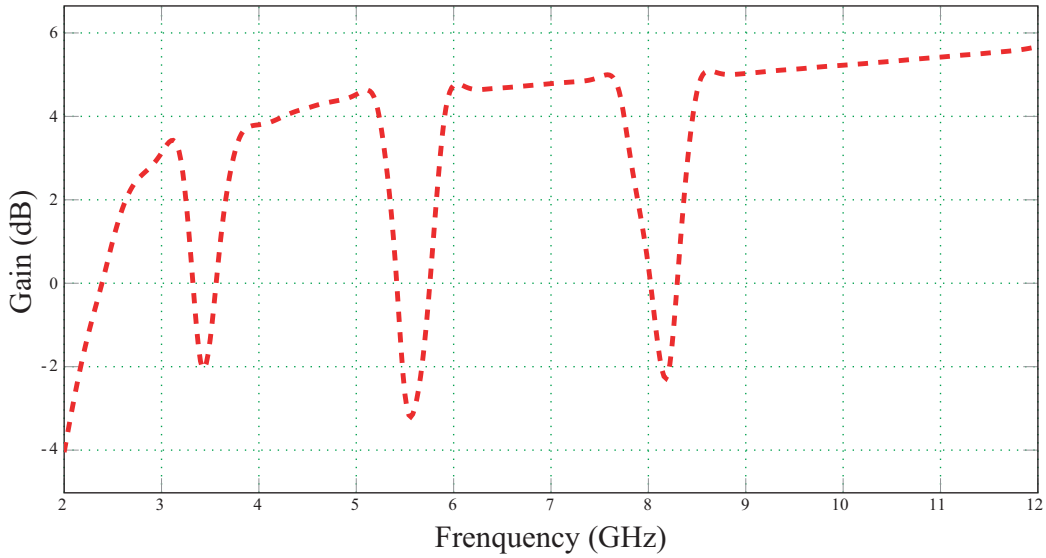

Figure 9. Simulated realized gain of UWB MIMO antenna.

antenna using the S-parameters is given below [48]:

$$ECC = \frac{|S_{11}^* S_{12} + S_{21}^* S_{22}|^2}{(1 - |S_{11}|^2 - |S_{21}|^2)(1 - |S_{22}|^2 - |S_{12}|^2)} \quad (1)$$

The value of ECC should ideally be zero for an uncorrelated MIMO antenna. However for practical circumstances, the preferred limit is ECC < 0.5. Figure 10 presents the graph of ECC versus frequency of the proposed UWB MIMO antenna. From the figure it is observed that the ECC < 0.02 for the proposed UWB MIMO antenna in the entire UWB range.

Diversity gain is also an important parameter to evaluate the diversity performance of the antenna.

The relation to calculate DG of the MIMO antenna is as given below:

$$DG = 10\sqrt{1 - (ECC)^2} \tag{2}$$

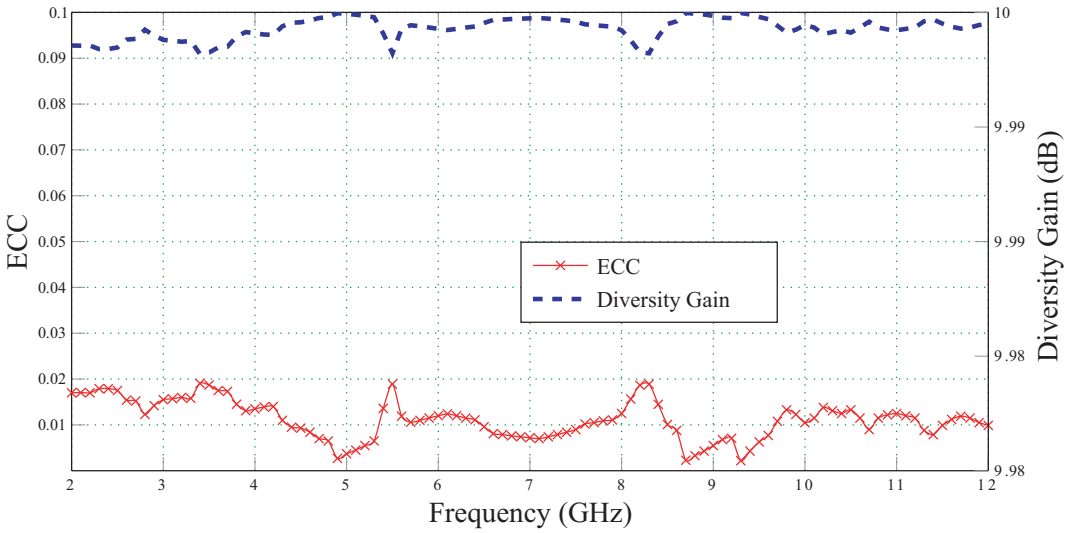

Figure 10. Plot of ECC and Diversity versus frequency for the proposed UWB MIMO antenna.

Table 2. Performance comparison of the proposed UWB MIMO antenna with previously published work.

Ref.	Freq range of antenna (GHz)	Area (mm^2)	No. of notched bands	No. of MIMO elements	Isolation (dB)	Isolation Technique
[29]	3.1–10.6	1400	–	Two	> 16	Tree like structure
[30]	2.8–8	3491	–	Two	> 17	Separated ground planes
[31]	3–6	3000	–	Two	> 21	Double layer EBG structure
[32]	3.4–15	1600	Two	Two	> 15	Polarization diversity with protruded stub
[33]	2.8–11.5	1400	One	Two	> 18	Pattern diversity
[34]	2.8–11	1260	One	Two	> 20	T-shaped stubs
[35]	2.4–14.5	1500	-	Two	> 20	F-shaped stubs
[36]	2.3–10.6	2610	Three	Two	> 15	Decoupling strips and slot in ground plane
[37]	3.1–12.3	1430	–	Two	> 20	Pattern diversity
[38]	31–12	2116	Two	Two	> 17	Minkowski fractal structure
[39]	3–11	1750	–	Two	> 25	Fence like decoupling structure
[40]	3–16	1472	Two	Two	> 20	Periodic strip branches
[41]	2.36–12	1724	Two	Two	> 21	Double Y-shaped branch
Proposed	2.5–12	1320	Three	Two	> 20	F-shaped stubs and slot in ground plane

The variation of DG of the proposed UWB MIMO antenna with frequency is also plotted in Figure 10. It is observed that the value of DG of the proposed UWB MIMO antenna is approximately 10 dB for the entire UWB frequency range.

6.4. Comparison with Other Reported Work

Table 2 compares the proposed UWB MIMO antenna with other UWB MIMO antennas reported in literature in terms of bandwidth, overall footprint of antenna, number of notched bands, isolation achieved, and the isolation technique used. In the comparison table, only two element MIMO antennas are taken so that a fair comparison of the area occupied by proposed antenna with other reported antennas can be made. It can be observed that the overall area of the proposed MIMO antenna is less than many of the reported antennas. Moreover, the proposed antenna exhibits acceptable bandwidth and good isolation between the individual antenna elements. The proposed antenna also rejects three interfering bands while using only a single cell of a triple bandgap CSRR-loaded EBG structure per antenna element. Additionally, the CSRR-loaded EBG structure is compact in size and easy to fabricate, as can be observed from Table 1.

7. CONCLUSION

In this paper, a compact two-element triple band-notched UWB MIMO antenna is proposed. The proposed MIMO antenna is fabricated and tested. The antenna offers a wide impedance bandwidth of 2.5–12 GHz. Three notches in the the UWB bandwidth are achieved by embedding single cell of a compact CSRR-loaded EBG structure near the feedline of UWB monopole antenna. From the measurement results, the notched bands are 3.43–3.86 GHz, 5.26–6 GHz, and 7.85–8.71 GHz. A mirrored pair of F-shaped stubs and a slot in the common ground plane of the MIMO antenna help in improving the isolation between MIMO elements. The MIMO antenna also exhibits good diversity performance with value of ECC < 0.02, and DG ≈ 10 dB for the entire UWB band.

REFERENCES

1. Federal Communications Commission (FCC), Washington DC, "First report and order in the matter of revision of Part 15 of the commissions rules regarding ultra-wideband transmission systems," ET-Docket 98–153, 2002.
2. Ghavami, M., L. B. Michael, and R. Kohno, "Ultra-wideband signals and systems in communication engineering," 2nd Edition, John Wiley & Sons, 2007.
3. Jung, J., W. Choi, and J. Choi, "A small wideband microstrip-fed monopole antenna," *IEEE Microw. Wireless Compon. Lett.*, Vol. 15, No. 10, 703–705, Oct. 2005.
4. Abbosh, A. M. and M. E. Bialkowski, "Design of ultra-wideband planar monopole antennas of circular and elliptical shape," *IEEE Trans. Antennas Propag.*, Vol. 56, No. 1, 17–23, Jan. 2008.
5. Wu, Q., R. Jin, J. Geng, and M. Ding, "Printed omni-directional UWB monopole antenna with very compact size," *IEEE Trans. Antennas Propag.*, Vol. 56, No. 3, 896–899, Mar. 2008.
6. Ojaroudi, M., G. Kohneshahri, and J. Noory, "Small modified monopole antenna for UWB application," *IET Microw. Antennas Propag.*, Vol. 3, No. 5, 863–869, Aug. 2009.
7. Ghaderi, M. R. and F. Mohajeri, "A compact hexagonal wide-slot antenna with microstrip-fed monopole for UWB application," *IEEE Antennas Wireless Propag. Lett.*, Vol. 10, 682–685, Jun. 2011.
8. Ahmed, O. and A. Sebak, "A printed monopole antenna with two steps and a circular slot for UWB applications," *IEEE Antennas Wireless Propag. Lett.*, Vol. 7, 411–413, Jun. 2008.
9. Dong, Y. D., W. Hong, Z. Q. Kuai, and J. X. Chen, "Analysis of planar ultra-wideband antennas with on-ground slot band-notched structures," *IEEE Trans. Antennas Propag.*, Vol. 57, No. 7, 1886–1893, Jul. 2009.
10. Li, W. T., X. W. Shi, and Y. Q. Hei, "Novel planar UWB monopole antenna with triple band-notched characteristics," *IEEE Antennas Wireless Propag. Lett.*, Vol. 8, 1094–1098, Oct. 2009.

11. Nguyen, T. D., D. H. Lee, and H. C. Park, "Design and analysis of compact printed triple band-notched UWB antenna," *IEEE Antennas Wireless Propag. Lett.*, Vol. 10, 403–406, Apr. 2011.
12. Nguyen, D. T., D. H. Lee, and H. C. Park, "Very compact printed triple band-notched UWB antenna with quarter wavelength slots," *IEEE Antennas Wireless Propag. Lett.*, Vol. 11, 411–414, Apr. 2012.
13. Kim, K.-H., Y.-J. Cho, S.-H. Hwang, and S.-O. Park, "Band-notched UWB planar monopole antenna with two parasitic patches," *Electron. Lett.*, Vol. 41, No. 14, 783–785, Jul. 2005.
14. Zaker, R., C. Ghobadi, and J. Nourinia, "Bandwidth enhancement of novel compact single and dual band-notched printed monopole antenna with a pair of L-shaped slots," *IEEE Trans. Antennas Propag.*, Vol. 57, No. 12, 3978–3983, Dec. 2009.
15. Hosseini, H., H. R. Hassani, M. H. Amini, "Miniaturised multiple notched omnidirectional UWB monopole antenna," *Electron. Lett.*, Vol. 54, No. 8, 472–474, Apr. 2018.
16. Zhu, F., S. Gao, A. T. S. Ho, et al., "Multiple band-notched UWB antenna with band-rejected elements integrated in the feed line," *IEEE Trans. Antennas Propag.*, Vol. 61, No. 8, 3952–3960, Aug. 2013.
17. Sarkar, D., K. V. Srivastava, and K. Saurav, "A compact microstrip-fed triple band-notched UWB monopole antenna," *IEEE Antennas Wireless Propag. Lett.*, Vol. 13, 396–399, Feb. 2014.
18. Yazdi, M. and N. Komjani, "Design of a band-notched UWB monopole antenna by means of an EBG structure," *IEEE Antennas Wireless Propag. Lett.*, Vol. 10, 170–173, Feb. 2011.
19. Peng, L. and C. Ruan, "UWB band-notched monopole antenna design using electromagnetic bandgap structures," *IEEE Trans. Microw. Theory Techn.*, Vol. 59, No. 4, 1074–1081, Mar. 2011.
20. Peng, L. and C. Ruan, "Design and time-domain analysis of compact multi-band-notched UWB antennas with EBG structures," *Progress In Electromagnetics Research B*, Vol. 47, 339–357, 2013.
21. Jaglan, N., B. K. Kanaujia, S. D. Gupta, and S. Srivastava, "Triple band notched UWB antenna design using electromagnetic band gap structures," *Progress In Electromagnetics Research C*, Vol. 66, 139–147, 2016.
22. Dalal, P. and S. K. Dhull, "Upper WLAN band notched UWB monopole antenna using compact two via slot electromagnetic band gap structure," *Progress In Electromagnetics Research C*, Vol. 100, 161–171, 2020.
23. Liu, H. and Z. Xu, "Design of UWB monopole antenna with dual notched bands using one modified electromagnetic-bandgap structure," *The Scientific World Journal*, Vol. 2013, 2013.
24. Pandey, G. K., H. S. Singh, P. K. Bharti, and M. K. Meshram, "Design and analysis of multiband notched pitcher-shaped UWB antenna," *Int. J. RF and Microwave Comp. Aid. Eng.*, Vol. 25, 795–806, 2015.
25. Ghosh, A., T. Mandal, and S. Das, "Design and analysis of triple notch ultra-wideband antenna using single slotted electromagnetic bandgap inspired structure," *Journal of Electromagnetic Waves and Applications*, Vol. 33, No. 11, 1391–1405, 2019.
26. Trimukhe, M. A. and B. G. Hogade, "Compact ultra-wideband antenna with triple band notch characteristics using EBG structures," *Progress In Electromagnetics Research C*, Vol. 93, 65–77, 2019.
27. Bhavarthe, P. P., S. S. Rathod, and K. T. V. Reddy, "A compact dual band gap electromagnetic band gap structure," *IEEE Trans. Antennas and Propag.*, Vol. 67, No. 1, 596–600, Jan. 2019.
28. Kapure, V. R., P. P. Bhavarthe, and S. S. Rathod, "A switchable triple-band notched UWB antenna using compact multi-via electromagnetic band gap structure," *Progress In Electromagnetics Research C*, Vol. 104, 201–214, 2020.
29. Zhang, S., Z. Ying, J. Xiong, and S. He, "Ultra wideband MIMO/Diversity antennas with a tree-like structure to enhance wideband isolation," *IEEE Antennas Wireless Propag. Lett.*, Vol. 8, 1279–1282, 2009.
30. Jusoh, M., M. F. Jamlos, M. R. Kamarudin, and F. Malek, "A MIMO antenna design challenges for UWB application," *Progress In Electromagnetics Research B*, Vol. 36, 357–371, 2012.

31. Li, Q., A. P. Feresidis, M. Mavridou, and P. S. Hall, "Miniaturized double layer EBG structures for broadband mutual coupling reduction between UWB monopoles," *IEEE Trans. Antennas and Propag.*, Vol. 63, No. 3, 1168–1171, Mar. 2015.
32. Zhu, J., B. Feng, B. Peng, et al., "Compact CPW UWB diversity slot antenna with dual band-notched characteristics," *Microw. Opt. Technol. Lett.*, Vol. 58, 989–994, 2016.
33. Ibrahim, A. A., J. Machac, and R. M. Shubair, "Compact UWB MIMO antenna with pattern diversity and band rejection characteristics," *Microw. Opt. Technol. Lett.*, Vol. 59, No. 6, 1460–1464, 2017.
34. Yadav, D., M. P. Abegaonkar, S. K. Koul, et al., "Two element band-notched UWB MIMO antenna with high and uniform isolation," *Progress In Electromagnetics Research M*, Vol. 63, 119–129, 2018.
35. Iqbal, A., O. A. Saraereh, A. W. Ahmad, and S. Bashir, "Mutual coupling reduction using F-shaped stubs in UWB MIMO antenna," *IEEE Access*, Vol. 6, 2755–2759, 2018.
36. Jaglan, N., S. D. Gupta, B. K. Kanaujia, et al., "Triple band notched DG-CEBG structure based UWB MIMO/diversity antenna," *Progress In Electromagnetics Research C*, Vol. 80, 21–37, 2018.
37. Toktas, A. and A. Akdagli, "Compact multiple-input multiple-output antenna with low correlation for ultra-wide-band applications," *IET Microw. Antennas Propagn.*, Vol. 9, No. 8, 822–829, 2015.
38. Debnath, P., A. Karmakar, A. Saha, and S. Huda, "UWB MIMO slot antenna with Minkowski fractal shaped isolators for isolation enhancement," *Progress In Electromagnetics Research M*, Vol. 75, 69–78, 2018.
39. Wang L., Z. Du, H. Yang, et al., "Compact UWB MIMO antenna with high isolation using fence-type decoupling structure," *IEEE Antennas Wireless Propag. Lett.*, Vol. 18, No. 8, 1641–1645, Aug. 2019.
40. Zhang, J., L. Wang, and W. Zhang, "A novel dual band-notched CPW-fed UWB MIMO antenna with mutual coupling reduction characteristics," *Progress In Electromagnetics Research Letters*, Vol. 90, 21–28, 2020.
41. Zhou, J.-Y., Y. Wang, J.-M. Xu, and C. Du, "A CPW-fed UWB-MIMO antenna with high isolation and dual band-notched characteristic," *Progress In Electromagnetics Research M*, Vol. 102, 27–37, 2021.
42. Jaglan, N., P. Dalal, S. D. Gupta, and M. A. Abdalla, "Band notched UWB MIMO/diversity antenna design with inductance boosted compact EBG structures," *Progress In Electromagnetics Research C*, Vol. 105, 185–202, 2020.
43. Ma, T. and S. Wu, "Ultrawideband band-notched folded strip monopole antenna," *IEEE Trans. Antennas and Propag.*, Vol. 55, No. 9, 2473–2479, Sept. 2007.
44. Yang, F. and Y. Rahmat-Samii, *Electromagnetic Band Gap Structures in Antenna Engineering*, Cambridge University Press, 2009.
45. Dalal, P. and S. K. Dhull, "Electromagnetic band gap structure applications in modern wireless perspective: A review," *IEEE Intl. Conf. Advances Comput. Commun. Eng.*, Sathyamangalam, India, Apr. 2019.
46. Dalal, P. and S. K. Dhull, "Eight-shaped polarization-dependent electromagnetic bandgap structure and its application as polarization reflector," *Intl. J. Microw. Wireless Technol.*, 1–9, 2021.
47. Peng, L., C. Ruan, and Z. Li, "A novel compact and polarization-dependent mushroom-type EBG using CSRR for dual/triple-band applications," *IEEE Microw. Wireless Compon. Lett.*, Vol. 20, No. 9, 489–491, Sept. 2010.
48. Blanch, S., J. Romeu, and I. Corbella, "Exact representation of antenna system diversity performance from input parameter description," *Electron. Lett.*, Vol. 39, No. 9, 705–707, May 2003.